

Performance Evaluation of IREDA Prototype System: An IR-Based Portable Electronic Detection System for Blood Alcohol Concentration

Panayiota Demosthenous^a, Kleanthis Erotokritou^b and Marios Sergides^c
Cy.R.I.C. Cyprus Research & Innovation Center Ltd, 28th October Avenue, 2414, Nicosia, Cyprus

Keywords: Ethanol Detection, Blood Alcohol Concentration (BAC), Breath Alcohol Concentration (BrAC), Transdermal Alcohol Concentration (TrAC), Tissue Alcohol Concentration (TAC), Near Infrared (NIR), Diffused Reflectance, Tissue Phantoms, Integrating Sphere, Touch-Based Detection, Gas-Based Detection.


Abstract: This paper demonstrates a prototype system called IREDA, which is an IR-based Portable Electronic Detection System for Blood Alcohol Concentration. IREDA examines, a) the feasibility on detecting Ethanol on human body via near-infrared diffused reflectance with a touch-based oriented detection, and b) the feasibility on detecting Ethanol in human respiration via multiple light absorptions with gas-based detection. IREDA has proved the feasibility on detecting ethanol vapour with limit of detection of about 12 mg/L, and the feasibility on detecting Ethanol in solid gelatine samples. Even though, it is challenging to compare these results with data alcohol consumption in humans, IREDA can be considered as a promising prototype towards this direction.


1 INTRODUCTION


Driving under the influence (DUI) of alcohol is responsible for the 25% of all road fatalities in the European Union. According to the European Commission Communication, efficient ways to control alcohol intake and advice users on their ability to drive are critical to prevent accidents. The need to indirectly monitor blood alcohol levels for safety, medical, legal or health reasons, as well as, for safe recreational alcohol consumption, led to several non-invasive solutions that use biofluid samples such as lacrimal fluid, saliva, sweat. Alternative methods consist of measuring breath alcohol concentration (BrAC) or tissue alcohol concentration (TAC).

Breathalyzers are widely used for indirectly determining BAC (Jurič, Fijačko, Bakulić, Orešić, & Gmajnički, 2018), but their resulting measurements usually suffer from inaccuracies due to interference from external and internal factors such as humidity, temperature, individuals' traits, subject physiological variations, contamination of mouth compounds and

environmental vapours. Two other methods, namely an eyeglasses-based tear biosensing device (Sempionatto, et al., 2019) and a saliva electrochemical ring sensor (Mishra, et al., 2020), use biofluid samples. However, the former involves tear stimulation, and the latter is missing pH and temperature sensors to compensate for temperature changes or variations in saliva pH. Moreover, there are several other transdermal alcohol sensing methods (Fairbairn & Kang, 2019) that detect either liquid or gas phases of alcohol just above the skin. However, detection in sweat can only be achieved if sweat is produced after a stimulation process, which in general introduces limitations. Furthermore, individual and environmental factors (e.g., skin thickness, gender differences, humidity, temperature) are introducing variations in transdermal alcohol readings, which also present late response with a time lag of a couple of hours. Finally, non-invasive optical methods exist for blood alcohol concentration measurements on tissue sample, among which, infrared spectroscopy (IR) was found to be the most

^a  <https://orcid.org/0000-0001-5088-9029>

^b  <https://orcid.org/0000-0002-7284-104X>

^c  <https://orcid.org/0000-0002-4344-4416>

promising, employing either near-infrared (Ver Steeg, et al., 2017) or mid-infrared spectrum (Guo, et al., 2018). Specifically, wavelength-modulated differential photothermal radiometry (WM-DPTR), has the capability of measuring BAC with high resolution at around 5 mg/dl and a low detection limit at around 10 mg/dl. However, this methodology is currently using laboratory equipment, presenting limitations on further miniaturization for personal use.

This work demonstrates a prototype system called IREDA, which is an IR-based Portable Electronic Detection System for Blood Alcohol Concentration. IREDA examines the feasibility of detecting blood alcohol (ethanol) in a) human body via near-infrared (NIR) diffused reflectance with a touch-based oriented detection (P. Demosthenous, Near Infrared Diffused Reflectance on Tissue Simulating Phantoms for Optical Applications., 2022), and b) in human respiration via multiple light reflection and absorption with gas-based detection (P. Demosthenous, Infrared Spectroscopic Application using an Integrating Sphere for Measuring Vapor Ethanol, 2022).

The main optical component of the system is an integrating sphere for the efficient collection of the diffused light from the sample. Integration spheres are known to be beneficial in spectroscopic applications (LM. Hanssen, 2022) and are used to enhance the collection of backscattered light in non-invasive sensing applications such as, finger photo plethysmography for determining blood concentration (T. Yamakoshi, 2015), and laser spectroscopy for glucose sensing (A. Werth, 2018). Likewise, integrating spheres are used in gas sensing applications, as they easily increase the effective optical path length from the light source to the detector. Hence, the interaction length between light and the gas sample becomes longer (S. Tranchart, 1996), increasing the sensitivity of the gas-based detection system. To examine NIR diffused reflectance on simulating tissues, the experiments use low-cost optical tissue phantoms (L. Ntombela, 2020) composed of water, gelatine, and titanium dioxide (TiO₂) powder. Such samples are commonly used in optical applications to mimic human tissue.

The following sections present the system implementation, as well as the experimental testing and results for the performance evaluation of IREDA.

2 SYSTEM IMPLEMENTATION

This section describes: a) the hardware architecture of the system, b) the optical setup and optoelectronics

that has been used, c) the system's software with the signal processing algorithm, and d) the overall system integration.

2.1 System's Hardware Architecture

There are several individual modules that are included in the hardware development of IREDA. These are a) the current driver, b) the temperature controller of the light sources, c) the transimpedance amplifier of the photodetector, and d) the main control unit (MCU) of the system. Figure 1 shows the architecture of the hardware electronic subsystem. This design presents all the connections between the specified peripherals and clarifies the communication protocols and the digital and analogue signals between them, as well as the power supply requirements.

A laser diode driver has been chosen to drive the NIR light sources at a constant current mode. This module can drive two independent outputs up to 250mA, controlled by two separate modulation signals. A temperature controller is used to set and control the temperature of the light sources, ensuring wavelength stability during optical measurements. A transimpedance amplifier was chosen, for the amplification of the photodetector signal. This amplifier converts photodiode's output current to voltage with a switchable gain from 1, 10 and 100 MV/A. A controller from National Instruments has been used as the MCU.

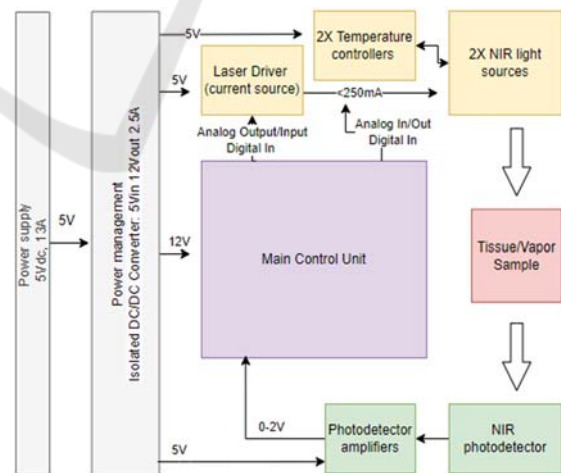


Figure 1: IREDA hardware architecture.

The MCU is responsible to control all the above peripherals, the laser driver, the TECs and the photodetector. Specifically, the MCU is used to set the optical intensity and wavelength of the NIR light sources, read the photodetector signal, and provide

the collected data to the 'data analysis software'. The optical intensity can be controlled via the laser driver that applies a constant or pulsed current through the lasers' anode and cathode. The laser wavelength can be controlled by changing the lasers' temperature using the temperature controller. While the light sources illuminate the sample, the photodetector collects the reflected radiation that gives information on ethanol presence within the sample. The photodetector signal is then digitized by an analogue-to-digital converter (ADC) on the MCU. The raw data are then provided to a custom-made LabVIEW data analysis software for further processing.

2.2 Optics and Optoelectronics

The optical setup described in this section is designed to accommodate two separate infrared light sources, which can be detected by a single photodetector. The schematic of the optical module used in IREDA, is shown in Fig. 2.

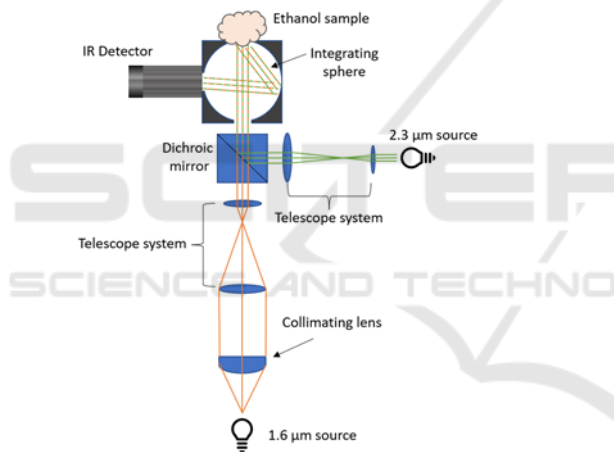


Figure 2: Schematic of IREDA optical apparatus.

This optical setup consists of two NIR sources at 1.6 μm and 2.3 μm . The former is a light emitting diode (LED) and it is connected to a temperature-controlled mount. The 2.3 μm source is a distributed feedback laser diode. Directly after the 1.6 μm LED source, a collimator lens is used. Subsequently, the collimated beam passes through an inversed telescope system ($\sim 20\times$) formed by two additional lenses to reduce the beam diameter to slightly less than 8 mm which is the port opening of the integrating sphere. In the path of the 2.3 μm source merely a telescope system is advised, consisting of 15 mm and 35 mm focal length lenses to increase the beam diameter. The two beams then arrive at a short pass dichroic mirror with cut-off wavelength at 1800 nm allowing for wavelengths shorter than 1800 nm to be

transmitted and longer wavelengths to be reflected. The combined beams then enter the integrating sphere and illuminate the sample mounted at the opposite port, the 'sample port'. The integrating sphere is chosen here to collect the light that is diffusely reflected by the sample at all angles, thus maximizing the detector's signal and increasing signal stability. As mentioned previously, the beam diameter from both light sources is reduced to be slightly smaller than the port diameter of the integrating sphere. This is done to allow the light to interact with a maximum area of the sample without being directly reflected by the inner walls of the sphere. An NIR detector is connected to the side port to measure light intensity as reflected by the sample. The fine adjustment of the two lens systems was achieved by leaving the top port open but in the absence of sample. Since both beams are collimated and with diameters slightly less than port size, the detected signal was almost null. The maximum device signal was detected when the top port was sealed with a reflective-coated plug.

A real image of the optical module is shown in Fig. 3. This optical setup, as described above, was designed as a touch-based detection system for ethanol detection in 'tissue' samples. At the same time, this setup can be used as a gas-based detection system for vapor ethanol detection, where multiple light reflections within the integrating sphere offer multiple absorption paths into the gas that fills the sphere. The difference in this case is that the top port of the sphere is kept closed with its reflective-coated plug, while the side port of the sphere now serves as the gas/vapor inlet port.

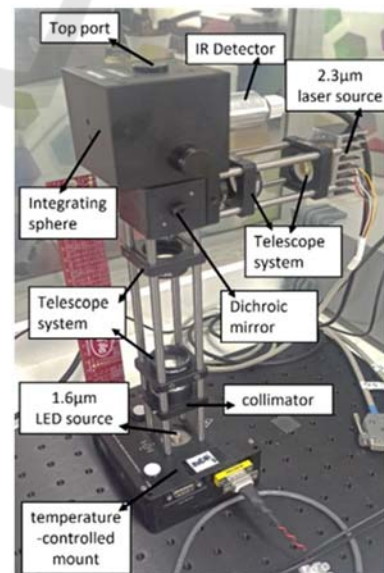


Figure 3: The optical setup of IREDA.

2.3 System Software-Signal Processing

During an optical measurement, both light sources are operated simultaneously and are modulated by a square waveform. To differentiate the signal originated by the two different light sources, one is modulated at 100 Hz and the other at double this value. The synchronous detection of the photodetector (PD) signal is done digitally by sampling the measured and modulation signals and processing them via the IREDA data analysis software. Figure 4 shows an example of the two modulated signals and the total PD signal which is a summation of the two. Furthermore, a digitally lock-in signal processing algorithm is implemented (M. Baer, 2021). Via this algorithm we managed simultaneous signal acquisition from two light sources, by synchronous detection of their modulation signals of orthogonal frequencies.

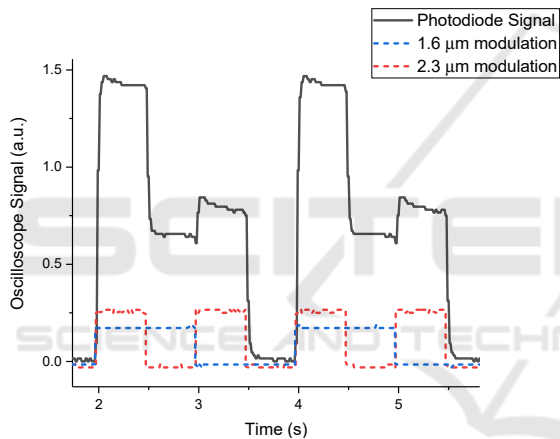


Figure 4: Example of the modulation and photodiode signals as measured via the oscilloscope signal.

The IREDA software is used to visualize the analyzed data in real time. The temperature control, current control and modulation of the light sources (LS) can be also accessed and modified by the software. The modulation of the two LSs can be visualized and verified by the real-time PD signal. Additionally, the signal corresponding to each individual LS as well as their ratio is displayed. When light is lost due to absorption or for example due an integrating sphere open port, there is a decrease observed in the individual LS signals.

2.4 System Assembly

The optical setup, the electronic hardware, and the data analysis software were integrated together within an acrylic enclosure to construct IREDA system.

Figure 5 presents the final integrated prototype system, indicating the main modules and optical components.

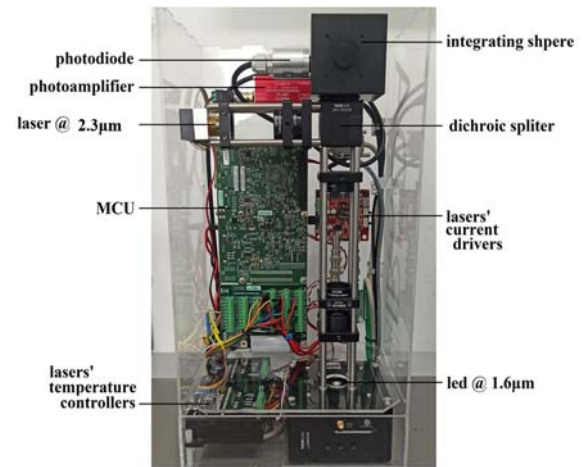


Figure 5: The integrated IREDA prototype.

3 EXPERIMENTAL TESTING AND RESULTS

This section describes the experimental validation of IREDA's performance, both as a) a touch-based and b) gas-based ethanol-detection system. Both cases used the same configuration parameters. The applied voltage to the 1.6 μm LED (LS1) source was set at 1 V, and 1.5 V for the 2.3 μm laser source (LS2), while the two sources were modulated at 0.1 kHz and 0.2 kHz respectively. The amplifier connected to photodiode detector was set to an amplification value of 10 MV/A.

3.1 Validation of the Gas-Based Detection System

3.1.1 Experimental Configuration Using Latex Balloon as the Vapour Provider

A latex balloon was used to provide the integrating sphere with a constant volume of ethanol vapour. A specific amount of liquid solution was added to the balloon prior inflation. The balloon was inflated to a diameter of approximately 20 ± 1 cm and sealed allowing the solution to evaporate for several seconds. Subsequently, it was connected to the "sample port" via a tube (Fig. 8) and the air-vapour mixture was released into the sphere. Due to the constant volume of air used in this method, an actual

sample concentration can be calculated by approximating the balloon volume to that of a sphere.

Data collection initiated prior connecting the balloon to the sample port to ensure zero absorption i.e., maximum PD signal. The balloon was then allowed to deflate resulting to PD signal drop due to absorption. Afterwards, the balloon was disconnected and allowed the system to “empty”. After observing maximum PD signal denoting “empty” sphere, an additional balloon with different ethanol concentration was connected. Figure 6 shows an example of a raw data sequence recorded in this set of experiments. Different regions represent time periods where the sphere contained no ethanol vapour (empty), was filled with vapour (filling) and finally exhausting the vapour again (emptying).

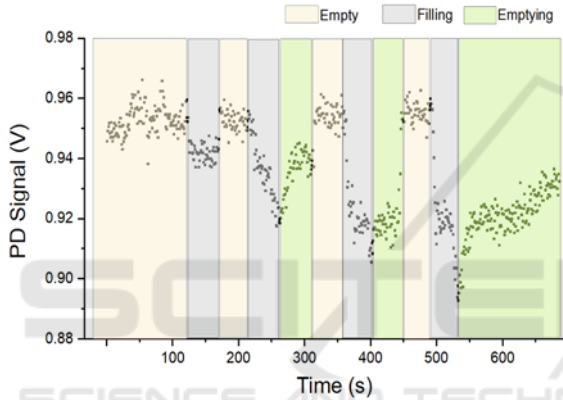


Figure 6: Example of photodiode signal. The different coloured time regions represent the process of ethanol vapour entering and exiting the integrating sphere.

Different concentrations of ethanol were investigated with this configuration, ranging from 15 – 240 mg/L. Figure 7 presents the normalised transient PD signal for both light sources. It was observed that increasing ethanol concentration resulted to a greater drop in PD signal for LS2, with a maximum decrease of 10% recorded for the highest concentration. In the case of LS1 the change in absorption was less significant.

The collected data confirmed the capability of the setup detecting alcohol vapour, while making it was possible to differentiate between different concentrations. Furthermore, lower concentrations of alcohol vapor needed to be evaluated to assess the limit of detection and to also compare to the functionality commercial devices.

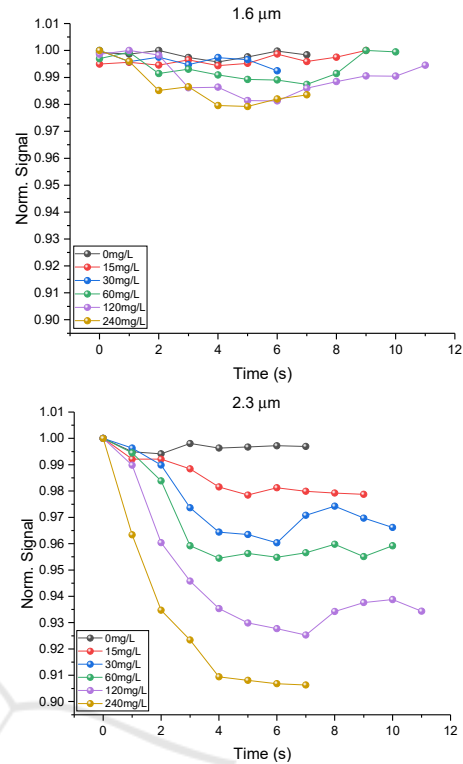


Figure 7: Normalised photodiode signal for (top) 1.6 μm and (bottom) 2.3 μm light sources, for different concentrations of ethanol vapour. Data presented here are up to the time where minimum PD signal was observed i.e., maximum absorption.

3.1.2 Experimental Configuration Using a Commercial Breathalyser

In order to compare the detection of gas ethanol in IREDA to a commercial device, a breathalyser was incorporated to the experimental setup. Additionally, the concentration calculation method was verified by this process. A split Y-tube was connected to the sample port so that the vapour from the latex balloon entered the breathalyser and the integrating sphere at the same time. An image of the modified experimental setup is shown in Figure 6.

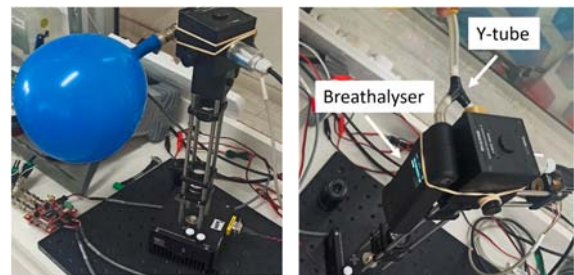


Figure 6: (left) Air-filled balloon connected to the setup, (right) modified experimental setup with a breathalyser.

The balloon sample was prepared in an identical manner to the previous experiments and connected to the Y-tube. Upon deflation the readings of the breathalyser and PD signal were recorded. It was noted that the breathalyser was saturated at about 14 μL of added liquid ethanol. A linear relation between the amount of ethanol added and the breathalyser reading was observed as shown in Figure 7. By fitting the data, a conversion factor from μL to mg/L of 0.172 $\text{mg/L}/\mu\text{L}$ was obtained, which agreed with the one derived by the concentration calculations for a 21 cm diameter sphere and 90% ethanol (0.171 $\text{mg/L}/\mu\text{L}$). It is noteworthy that the PD signal was indistinguishable for these lower concentration values (Figure 8).

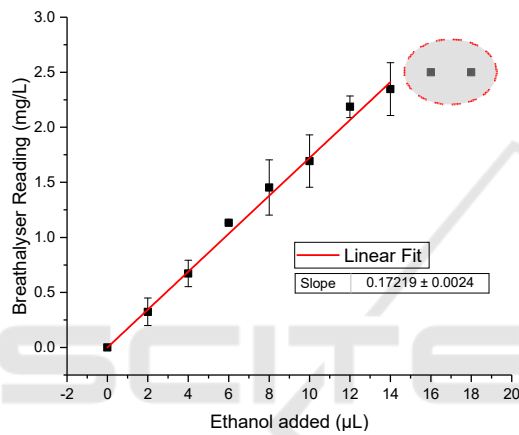


Figure 7: Breathalyser reading versus volume of ethanol added to the latex balloon. The breathalyser saturated for values over 14 μL (dashed red circle). The red solid line represents the linear fit of the data giving a conversion factor of 0.172 $\text{mg/L}/\mu\text{L}$.

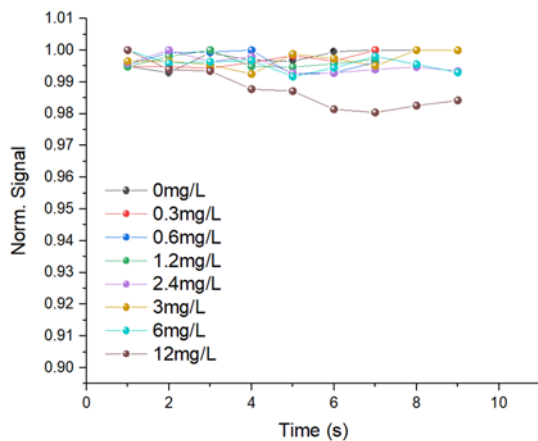


Figure 8: Normalised PD signal of the 2.3 μm laser source for lower ethanol concentrations between 0 and 12 mg/L . No notable change in signal was observed for concentrations below 12 mg/L .

The minimum concentration that the apparatus was able to detect was 12 mg/L of ethanol vapour. Furthermore, the signal for LS1 presented relatively minor changes for different concentrations and for this reason the data is omitted here. It can be concluded that the IREDA setup in its present form has an alcohol vapour detection limit of about 12 mg/L which is in the range of the upper limit of some commercial breathalysers.

3.1.3 Experimental Configuration Using an Air-Pressure Regulator Valve

To further optimize the setup, a pressure regulator was added between the balloon and the integrating sphere. This offered a controlled flow of gas mixture and granted monitoring light absorption as the integrating sphere was slowly filled. The regulator was set at a constant pressure of 0.2 bar. This eliminated the problem of the ethanol vapour mixture entering and exiting the sphere in an uncontrolled fashion thus creating inconsistencies between measurements. As the sample vapour was flowing into the sphere, the photodiode signal was decreased, eventually reaching a minimum value. As the sphere was filled with ambient air, absorption decreased, resulting to an increased photodiode signal.

The experiments were again divided into two concentration groups, low and high. The first one ranged from 0 – 7.5 mg/L with an additional high concentration of 30 mg/L for testing purposes, while the second group consisted of higher concentrations ranging from 0 – 120 mg/L . Figure 9 presents the normalised signal at 2.3 μm for both groups. Data presented here are up to 45 s; after this time frame the photodiode signal started increasing. Similar to the previous measurements, a noticeable drop in PD signal for high concentrations was observed but not in the case of the lower values. Nevertheless, the incorporation of the regulator to the setup allowed for the collection of a greater number of data points during each run which also revealed fluctuations in the signal over time.

Afterwards, the repeatability of data collection was assessed for a longer period. For these measurements, a latex balloon was filled with a certain amount of ethanol and deflated through the regulator. The integrating sphere was then flashed with ambient air and then filled again with the same concentration of ethanol vapour. This was repeated three times for each concentration, and it was found that repeated measurements were consistent. The average minimum signal value for each concentration was then derived. The same procedure was carried for

the zero concentration data points. A plot of the average signal versus concentration revealed a linear relationship (Figure 10), which in turn gave the rate of signal decrease with concentration, and it was found to be $-0.0013 \text{ (mg/L)}^{-1}$ which can be considered as the sensitivity of the device.

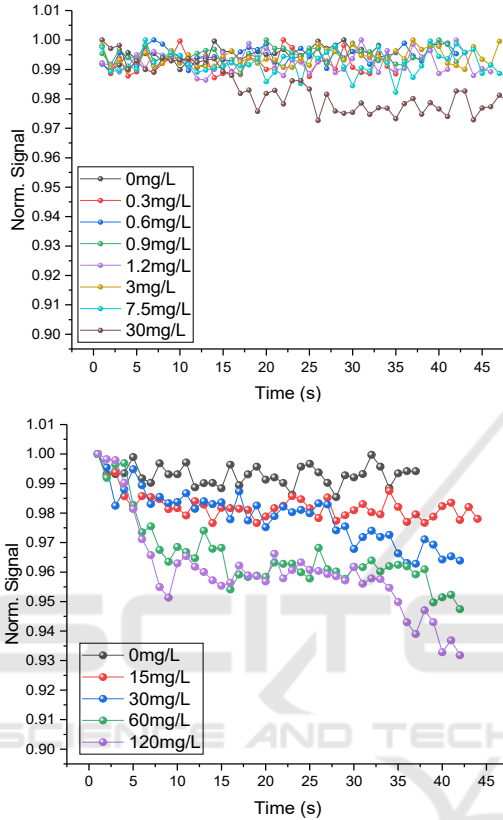


Figure 9: Normalised PD signal of the $2.3 \mu\text{m}$ laser source for (top) lower and higher (bottom) ethanol concentrations while the ethanol vapour flow was controlled by a pressure regulator set at 0.2 bar.

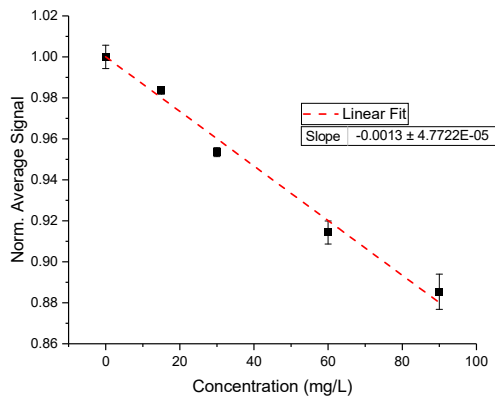


Figure 10: Average of the minimum signal versus ethanol concentration. The dashed red line is the linear fit of data.

3.2 Touch-Based Detection System Validation with Gelatine Samples

Subsequently, alcohol vapour was replaced by a gelatine mixture to test the device operation with solid samples resembling human tissue. Gelatine was the best candidate since it possesses similar properties with human tissue, it is easily accessible and low-cost. A generic gelatine powder used for cooking purposes was used in the following experiments. The samples were prepared by mixing gelatine powder with water and TiO_2 . The mixture was shaken for 5 minutes, microwaved for 20 seconds, and rotated on a carousel for 20 minutes. Afterwards, the mixture was poured in shallow round plastic containers (volume = 2.5 ml) and allowed to thicken and cool to room temperature (25°C). The sample was placed at the top port so the incoming light from the sources was directly incident on the gelatine while a known amount of ethanol was injected to gelatine via syringe. Data was collected on individual samples by increasing the injected ethanol after a period. At some point, the sample was allowed to relax so the ethanol was completely evaporated as shown in Figure 11. This was done to test that the signal returns to maximum (no absorption) while using the same sample in the absence of ethanol. The results revealed that by increasing the injected amount of ethanol in gelatine the LS2 signal further decreased. Even though a thorough comparison between these results and data involving real human tissue and alcohol consumption cannot be claimed, it is evident that the IREDA setup can detect changes in ethanol concentration present in solid samples.

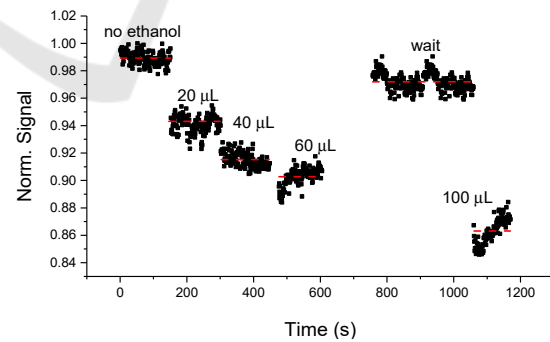


Figure 11 : Normalised PD signal of the $2.3 \mu\text{m}$ laser source for added injected ethanol volume in gelatine samples. Dashed red lines represent the average values.

4 CONCLUSIONS

IREDA has proved the ability to detect ethanol vapour that simulate human respiration, via multiple

light absorptions within an integrating sphere, leading to a gas-based detection setup with limit of detection of about 12 mg/L. Moreover, the feasibility on detecting ethanol in solid gelatine samples that simulate 'tissue' samples, via touch-based oriented detection and NIR diffused reflectance has been demonstrated. Even though, it is challenging to compare these results with data alcohol consumption in humans, IREDA can be considered as a promising prototype towards this direction.

ACKNOWLEDGEMENTS

The work was supported by the Project POST-DOC/0718/0186 which is co-financed by the European Regional Development Fund and the Republic of Cyprus through the Research and Innovation Foundation.

REFERENCES

- A. Werth, S. L. (2018). Implementation of an integrating sphere for the enhancement of noninvasive glucose detection using quantum cascade laser spectroscopy. *Applied Physics B*, 1-7.
- Fairbairn, C., & Kang, D. (2019). Temporal Dynamics of Transdermal Alcohol Concentration Measured via New-Generation Wrist-Worn Biosensor. *Alcoholism: Clinical and Experimental Research*, 2060-2069.
- Guo, X., Shojaei-Asanjan, K., Zhang, D., Sivagurunathan, K., Sun, Q., Song, P., . . . Zhou, Q. (2018). Highly sensitive and specific noninvasive in-vivo alcohol detection using wavelength-modulated differential photothermal radiometry. *Biomedical Optics Express*, 4638-4648.
- Jurič, A., Fijačko, A., Bakulić, L., Orešić, T., & Gmajnički, I. (2018). Evaluation of breath alcohol analysers by comparison of breath and blood alcohol concentrations. *Archives of Industrial Hygiene and Toxicology*, 69-76.
- L. Ntombela, B. A. (2020). Low-cost fabrication of optical tissue phantoms for use in biomedical imaging. *Heliyon*, e03602.
- LM. Hanssen, K. S. (2022). *Handbook of Vibrational Spectroscopy: Integrating spheres for mid-and near-infrared reflection spectroscopy*. John Wiley & Sons.
- M. Baer, B. S. (2021). Simultaneous Signal Acquisition by Synchronous Detection of Orthogonal Frequency Components. *Proceedings of SMSI 2021 Conference - Sensor and Measurement Science International*, 254-255.
- Mishra, R., Sempionatto, J., Li, Z., Brown, C., Galdino, N., Shah, R., . . . Tapert, S. (2020). Simultaneous detection of salivary Δ^9 -tetrahydrocannabinol and alcohol using a Wearable Electrochemical Ring Sensor. *Talanta*, 120757.
- P. Demosthenous, M. B. (2022). Infrared Spectroscopic Application using an Integrating Sphere for Measuring Vapor Ethanol. *Proceedings of OPAL 2022 - 5th International Conference on Optics, Photonics and Lasers*, 15-17.
- P. Demosthenous, M. B. (2022). Near Infrared Diffused Reflectance on Tissue Simulating Phantoms for Optical Applications. *Proceedings of OPAL 2022 - 5th International Conference on Optics, Photonics and Lasers*, 12-14.
- S. Tranchart, I. B. (1996). Sensitive trace gas detection with near-infrared laser diodes and an integrating sphere. *Applied optics*, 7070-7074.
- Sempionatto, J., Brazaca, L., García-Carmona, L., Bolat, G., Campbell, A., Martin, A., . . . Kim, J. (2019). Eyeglasses-based tear biosensing system: Non-invasive detection of alcohol, vitamins and glucose. *Biosensors and Bioelectronics*, 161-170.
- T. Yamakoshi, J. L. (2015). Integrating sphere finger-photoplethysmography: preliminary investigation towards practical non-invasive measurement of blood constituents. *PloS one*, e0143506.
- Ver Steeg, B., Treese, D., Adelante, R., Kraintz, A., Laaksonen, B., Ridder, T., . . . Hildebrandt, L. (2017). Development of a Solid State, Non-Invasive, Human Touch Based Blood Alcohol Sensor. In *Proceedings of 25th International Technical Conference on the Enhanced Safety of Vehicles*.